

## REMARKS

### Summary of Office Action

Examination of claims 16-31 is reported in the present Office Action. Claims 16-20, 22-25, and 27-31 are rejected under 35 U.S.C. § 112, first paragraph. Claims 16-31 are further rejected under 35 U.S.C. § 112, second paragraph. The rejections were addressed in the interview with the Examiner on October 3, 2003. The remaining issues are addressed below.

### Summary of Invention

The invention features methods of screening for compounds that may be useful for the treatment of Alzheimer's Disease. These methods stem from Applicants' discovery that endocytic pathway abnormalities in sporadic Alzheimer's disease identify the disease at a very early stage and likely alter amyloid precursor protein processing.

### Rejection under 35 U.S.C. § 112, first paragraph

Claims 16-20, 22-25, and 27-31 are rejected under 35 U.S.C. § 112, first paragraph, as lacking enablement. The claims feature methods of compound screening that require measuring the activity of an endocytic pathway in a cell overexpressing a rab5 nucleic acid.

During the interview conducted with the Examiner on October 3, 2003, the Examiner expressed two concerns: i) whether endosomal enlargement as described in the

Declaration of Dr. Nixon, filed on January 8, 2003, correlates with changes in endosomal activity recited in claims 17 and 28; and ii) whether the specification teaches *in vivo* screening methods. Each of these concerns is addressed below.

#### Correlation of Endosomal Enlargement and Endosomal Fusion

As requested by the Examiner, applicants submit herewith a Declaration of Dr. Ralph Nixon stating that a correlation exists between endosomal enlargement and endocytic activity, and more specifically, endosomal fusion.

At paragraph 4 of the Declaration, Dr. Nixon states that experiments carried out under his direction demonstrate that cells with enlarged endosomes also have increased endocytic pathway activity, which is characterized by specific endosomal changes (e.g., increased endosomal fusion, endosomal recycling, expression of MPR46, accumulation of lysosomal hydrolases in early endosomes, and accumulation of A $\beta$  in early endosomes) indicative of cells that are destined to be diseased in patients having Alzheimer's disease. In addition, Dr. Nixon states that rab5 overexpressing cells *in vitro* and *in vivo* mimic the increased endocytic pathway activity that is observed in patients with early stage Alzheimer's disease. As such, rab5 overexpressing cells are predicted to be useful in identifying compounds that modulate endosomal changes observed early in Alzheimer's disease. Such compounds are excellent potential therapeutics given that they are likely to be useful in treating patients at a time when patients are essentially asymptomatic.

In addition, Dr. Nixon describes experiments, at paragraph 5 of the Declaration, that were also disclosed in applicants' specification at page 16, line 7, to page 17, line 5. Dr. Nixon found that cells overexpressing rab5 had enlarged endosomes, similar to those observed in neurons from individuals with sporadic Alzheimer's Disease. In addition, a cDNA encoding the GTP-hydrolysis deficient rab5 mutant Q79L (Stenmark et al., EMBO J. 13:1287-1296, 1994) was expressed in L cells. Expression of the rab5 Q79L mutant resulted in increased endocytosis and the fusion of early endosomes into large vacuoles. Confirming that rab5 expression led to abnormal activity of the endosomal pathway, Dr. Nixon also demonstrated both increased uptake of fluid phase markers (FITC-dextran) and increased receptor mediated endocytosis (transferrin).

At paragraph 6 of the Declaration, Dr. Nixon states that experts accept that the presence of enlarged endosomes correlates with other markers of increased endocytic pathway activity, including endosomal fusion as evidenced in Roberts et al. (J. Cell Science 112:3667-3675, 1999).

At paragraph 7, Dr. Nixon states that Roberts et al. show that the presence of enlarged endosomes correlates with other markers of endosomal change, including endosomal fusion. Roberts overexpressed either wild-type rab5 or rab5:Q79L, a constitutively active rab5 mutant, in CHO and BHK cells and observed that the cells formed enlarged cytoplasmic vesicles that exhibited the characteristics of early endosomes. Using time-lapse video microscopy, Roberts showed that the enlarged endosomes resulted from endosomal fusion (page 3667, left column, abstract).

Regarding these results, Roberts states, “Time-lapse video microscopy shows the enlarged endosomes arise primarily by fusion of smaller vesicles. These fusion events occur mostly by a “bridge’ fusion mechanism in which the initial opening between vesicles does not expand; instead, membrane flows slowly and continuously from the smaller to the larger endosome in the fusing pair. . .”

At paragraph 8, Dr Nixon states that in sum, he has shown and experts accept that cells having enlarged endosomes also exhibit increased endocytic pathway activity, which is characterized by specific endosomal changes (e.g., increased endosomal fusion, endosomal recycling, expression of MPR46, accumulation of lysosomal hydrolases in early endosomes, and accumulation of A $\beta$  in early endosomes).

#### *In vivo* Compound Screening Methods

During the interview, the Examiner questioned whether applicants’ specification enables *in vivo* methods of compound screening. In particular, whether applicants’ specification teaches the methods recited in claims 17 and 28, which require measuring endosomal fusion, endosomal recycling, expression of MPR46, accumulation of lysosomal hydrolases in early endosomes, and accumulation of A $\beta$  in early endosomes of rab5 transgenic mice. As detailed below, methods for measuring the activity of an endocytic pathway *in vivo*, as recited in claims 17 and 28, are described in applicants’ specification.

### *Endosomal fusion and recycling*

At page 4, lines 2-6, applicants teach that endosomal fusion and endosomal recycling can be detected using compartment specific markers.

Using compartment-specific markers to identify early endosomes (rab5) combined with markers of endosomal fusion (rabaptin 5, early endosomal antigen EEA 1) and recycling (rab4), we have shown an upregulation of both endosomal fusion and recycling, indicating increased EP [endocytic pathway] activation.

In addition, applicants teach that such methods are useful in compound screening and may be carried out either on cells in culture or in the tissues of transgenic mice (page 31, lines 21-23, and page 7, lines 3-8).

### *Expression of MPR46*

Methods for detecting the accumulation of MPR46 in cells in culture are described at pages 14 and 15, under the heading “Example 3: Transfected cell models of endosomal and hydrolase trafficking abnormalities in AD brain,” where applicants describe methods for detecting MPR46 using immunofluorescence labeling (Figures 5A-5D), and at page 33, lines 11-16, where applicants teach that such methods can be used to assess the effects of candidate compounds administered to transgenic mice.

### *Accumulation of lysosomal hydrolases*

Methods for detecting lysosomal hydrolases (e.g., rab5, Cat D, and Cat B) in early endosomes are described at pages 32 and 33 under the heading “Localization of lysosomal hydrolases to early endosomes.” Applicants teach that antibodies that specifically recognize rab5, CatD, and CatB may be used to localize lysosomal

hydrolases to early endosomes in cells in culture or in transgenic mice. With respect to the use of transgenic mice in compound screening, applicants state:

A mouse from a transgenic line that is administered a candidate compound is analyzed to determine whether it exhibits evidence of decreased endocytosis or less mistrafficking of hydrolases to early endosomes compared to a transgenic mouse from the same line but not given a candidate compound. This can be performed using any of the assays described herein. In one example, sections of mouse brain are assessed by labeling with antibodies to rab5, CadD, and MPR46 (page 33, lines 11-16).

#### *Accumulation of A $\beta$*

Methods for detecting the accumulation of A $\beta$  in early endosomes are described, for example, at page 20, where applicants teach that immunocytochemical techniques were used to detect anti-A $\beta$  in neurons of segmental trisomy 16 (Ts65Dn) mice, an established model of human translocation Down's syndrome, as well as in postmortem human brain tissue obtained from patients with Down's syndrome and Alzheimer's Disease. These tissue samples also exhibited enlarged endosomes. Applicants state:

Using mice with segmental trisomy 16 (Ts65Dn). . . we found that, at two months of age and prior to the appearance of any neuropathological alterations, many neurons in the neocortex and basal forebrain contained enlarged early endosomes similar to those seen in AD and DS brain. . .

We found in Ts65Dn mice increased neuronal content of APP and the presence of intraneuronal A $\beta$  within vesicular compartments (Fig. 9). An antibody directed to the 17-24 region of the A $\beta$  peptide was used to probe brain tissue from the Ts65Dn mouse (Fig. 9B), as well as postmortem brain tissue from the neocortex of cases of human fetal, infant, and young DS, and cases obtained from adult patients in the very early stages of AD.

Using immunocytochemical techniques and light or confocal microscopy, we found the presence of small and discrete deposits of anti-A $\beta$  immunoreactive material within neurons of the Ts65Dn mice, the early stage DS cases and the cases in the earliest stages of AD (page 19, line 20, to page 20, line 15).

In sum, applicants' specification clearly discloses *in vivo* methods for measuring endosomal fusion, endosomal recycling, expression of MPR46, accumulation of lysosomal hydrolases in early endosomes, and accumulation of A $\beta$  in early endosomes of rab5 transgenic mice and the use of such methods in compound screening.

Rejection under 35 U.S.C. § 112, second paragraph

Claims 16-31 were rejected as indefinite for reciting "a compound that is useful for the treatment of Alzheimer's disease. As suggested by the Examiner, the amended claims recite "a compound that may be useful for the treatment of Alzheimer's disease."

CONCLUSION

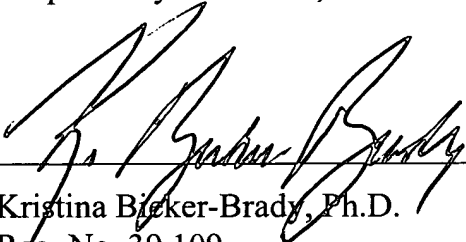
Enclosed is a Petition to extend the period for replying to the final Office action for 3 months, to and including October 9, and a check in payment of the required extension fee.

If there are any additional charges or any credits, please apply them to Deposit Account No. 03-2095.

Respectfully submitted,

Date:

October 9, 2003

  
\_\_\_\_\_  
Kristina Bieker-Brady, Ph.D.  
Reg. No. 39,109

Clark & Elbing LLP  
101 Federal Street  
Boston, MA 02110  
Telephone: 617-428-0200  
Facsimile: 617-428-7045



## Endosome fusion in living cells over expressing GFP-rab5

R. L. Roberts<sup>1</sup>, M. A. Barbieri<sup>1</sup>, K. M. Pryse<sup>2</sup>, M. Chua<sup>1</sup>, J. H. Morisaki<sup>1</sup> and P. D. Stahl<sup>1,\*</sup>

<sup>1</sup>Department of Cell Biology and Physiology and <sup>2</sup>Biochemistry and Molecular Biophysics, Washington University, School of Medicine, St Louis, MO, 63110, USA

\*Author for correspondence

Accepted 26 July; published on WWW 18 October 1999

### SUMMARY

CHO and BHK cells which overexpress either wild-type rab5 or rab5:Q79L, a constitutively active rab5 mutant, develop enlarged cytoplasmic vesicles that exhibit many characteristics of early endosomes including immunoreactivity for rab5 and transferrin receptor. Time-lapse video microscopy shows the enlarged endosomes arise primarily by fusion of smaller vesicles. These fusion events occur mostly by a 'bridge' fusion mechanism in which the initial opening between vesicles does not expand; instead, membrane flows slowly and continuously from the smaller to the larger endosome in the fusing pair, through a narrow, barely perceptible membranous 'bridge' between them. The unique aspect of rab5 mediated 'bridge' fusion is the persistence of a tight constriction at the site where vesicles merge and we hypothesize that this constriction results from the relatively slow disassembly of a putative docking/fusion complex. To determine the relation of rab5 to the fusion 'bridge', we used confocal fluorescence microscopy to monitor endosome fusion in cells overexpressing GFP-rab5 fusion proteins. Vesicle docking

in these cells is accompanied by recruitment of the GFP-rab5 into a brightly fluorescent spot in the 'bridge' region between fusing vesicles that persists throughout the entire length of the fusion event and which often persist for minutes following endosome fusion. Other endosomal membrane markers, including FM4-64, are not concentrated in fusion 'bridges'. These results support the idea that the GFP-rab5 spots represent the localized accumulation of GFP-rab5 between fusing endosomes and not simply overlap of adjacent membranes. The idea that the GFP-rab5 spots do not represent membrane overlap is further supported by experiments using photobleaching techniques and confocal imaging which show that GFP-rab5 localized in spots between fusion couplets is resistant to diffusion while GFP-rab5 on endosomal membranes away from these spots rapidly diffuses with a rate constant of about  $1.0 (\pm 0.3) \times 10^{-2} \text{ cm}^2/\text{second}$ .

Key words: Endosome, Fusion, rab5, Green fluorescent protein

### INTRODUCTION

The vacuolar apparatus is a system of internal membranes that separate eukaryotic cells into a number of functionally distinct compartments that organize essential cellular processes including endocytosis and exocytosis. In endocytosis, bits of the plasma membrane, including receptors with bound ligand, are internalized by endocytic vesicles. The vesicles are incorporated into the endosomal compartment where a number of sorting events occur, including the separation and segregation of recycling receptors from their respective ligands (Gruenberg and Maxfield, 1995). Incorporation of endocytic vesicles into the sorting endosomal compartment requires the close apposition of these compartments, a vesicle docking reaction, and membrane fusion. Two classes of vesicle membrane proteins have been proposed to participate in vesicle docking reactions and include the SNAREs (Hay and Scheller, 1997; Rothman and Warren, 1994) and the rab family of small GTPases (Novick and Zerial, 1997). SNAREs assemble into stable complexes and it is this property which has led to the proposal that SNAREs play a critical role in vesicle docking (Söllner et al., 1993). However, a number of more recent

studies have demonstrated a post-docking role for SNAREs in cells (Broadie et al., 1995; Hunt et al., 1994) and in liposome fusion reactions in vitro (Weber et al., 1998). The mechanism by which rabs promote vesicle docking is currently not known although in yeast it has been shown that a rab homologue is required for the assembly of SNARE complexes (Sögaard et al., 1994). Each of the many different rab proteins appears to operate at a single transport step and this property is consistent with a role of rab proteins in the regulation of SNARE pairing (Simons and Zerial, 1993).

Rab5 has been the focus of much recent work and is an important regulator of early endosome fusion (Barbieri et al., 1996; Stenmark et al., 1994). Endosome fusion has been reconstituted in vitro (Diaz et al., 1988) and is maximally stimulated by a GTPase-deficient rab5 mutant, rab5:Q79L (Barbieri et al., 1996; Stenmark et al., 1994) but the precise step that is regulated by rab5 is unknown.

Numerous reports utilizing time-lapse microscopic techniques have noted that fusion among endocytic vesicles occurs in a variety of cell types including macrophages (Lewis, 1931) and fibroblasts (Willingham and Yamada, 1978). However, none of these reports have included a detailed

morphological description of the membrane merger process as it occurs in endosome fusion nor has rab5 been localized in endosome docking and fusion reactions. Overexpression of rab5 in cells results in the formation of giant endosomal vesicles, as seen by light microscopy (Stenmark et al., 1994); however, the process by which these vesicles form is unknown. Here, we report our observations on the development of enlarged endosomes, as viewed by time-lapse light microscopy, using phase contrast and confocal imaging modes, in cells overexpressing wild type or a constitutively active rab5 mutant (rab5:Q79L). These studies have allowed us to distinguish two different types of membrane fusion, 'bridge' fusion and 'explosive' fusion. Additionally, localization studies in cells overexpressing GFP-rab5 fusion protein constructs show that endosome docking occurs as rab5 is recruited into a highly fluorescent spot in the contact zone between fusing endosomes and this occurs in both types of fusion. The localized accumulation of rab5 at the docking/fusion site suggests that a rab5-containing complex participates in endosome docking/fusion reactions.

## MATERIALS AND METHODS

### C II culture and reagents

The light microscopy described utilized either baby hamster kidney (BHK) cells or TRvb1 cells, a line of Chinese hamster ovary (CHO) cells that stably overexpress the human transferrin receptor. The latter cell line was generously supplied by Dr Tim McGraw (Columbia University, New York City, NY). Viral infection with recombinant Sindbis virus was done as described previously (Li and Stahl, 1993). After infection cells were maintained in media containing 1% fetal calf serum. Rhodamine-transferrin was prepared with carboxytetramethyl-rhodamine succinimidyl ester (Molecular Probes) by the method suggested by the manufacturer.

### Construction of GFP-rab5 fusion proteins

A cDNA of the GFP construct (GFP:S65T) used in these studies was amplified by 25 cycles of PCR (Heim et al., 1994). The 5' oligonucleotide contained an *Xba*I linker and the 3' primer contained a polylinker including restriction sites for *Hind*III, *Cla*I, *Sal*I and *Xba*I. The resulting PCR product was digested with *Xba*I and ligated into the unique *Xba*I site of the shuttle vector pH3'2J1. The GFP-rab5:wt and GFP-rab5:Q79L cDNA (Li and Stahl, 1993) were amplified by PCR using 5' and 3' oligonucleotide primers that contained *Hind*III and *Xba*I sites, respectively. The PCR products were then digested with *Hind*III and *Xba*I and purified by agarose gel electrophoresis. The rab5 primers were designed so that after ligation, the rab5 protein sequence fused in frame to the C terminus of GFP. Finally, the GFP-rab5 fusion constructs were excised from pH3'2J by *Xba*I/*Xho*I digestion and ligated into the *Xba*I/*Xho*I site of the Sindbis virus vector Toto 1000:3'2J.

### Time-lapse video and confocal microscopy

BHK and TRvb1 cells grown on glass coverslips were inverted on glass slides made into a narrow flow-cell by two strips of vacuum grease (Heuser et al., 1993) and were examined by either phase contrast or confocal microscopy. For phase contrast microscopy, cells were viewed with a  $\times 63$ , 1.4 NA phase contrast objective and photographed with a Hamamatsu video camera (model 2400 SIT; Hamamatsu Photonic Sys. Corp. Bridgewater, NJ) coupled through an Argus 10 image processor to a Panasonic TQ3038F optical memory disk recorder (OMDR). Mounted coverslips were warmed to 32–37°C with heating lamps. Time-lapsed confocal microscopy was carried out on a Bio-Rad MRC1024 confocal microscope using a  $\times 63$ , 1.4 NA

bright field objective and fluorescence and rhodamine filter sets. Confocal sequences were collected as Bio-Rad Pic files and were converted to bitmaps for use in Photoshop 3.0 and pixel intensity was quantitated. Determination of pixel intensity was done in experiments where images were collected with non-saturating conditions setup by the use of an output LUT. Photobleaching using the confocal laser was done as described by Cole et al. (1996).

### Membrane distribution, prenylation and GTP binding of GFP-rab5 fusion proteins

BHK cells were infected with Sindbis virus encoding GFP-rab5:wt or GFP-rab5:Q79L for 6 hours. After infection, a post-nuclear supernatant was prepared as described (Barbieri et al., 1996). Cytosol was prepared by centrifuging the post-nuclear supernatant at 10,000 *g* for 15 minutes at 4°C, and then centrifuging this supernatant at 30,000 *g* for 30 minutes at 4°C. All pellets were mixed and resuspended in the original volume (500  $\mu$ l). Equal amounts of cytosol and membrane were analyzed in SDS-PAGE. The distribution of rab5 in cytosol and membrane fractions was analyzed by western blotting using a mouse anti-rab5 monoclonal antibody generously supplied by Dr Angela Wandinger-Ness (Northwestern University, Chicago, IL), and a HRP-conjugated goat anti-mouse secondary antibody (Cappel). Positive staining was visualized by the ECL method (Amersham). The GTP binding blot was carried out as described (Barbieri et al., 1996) using a polyclonal anti-rab5 antibody (Santa Cruz Biotechnology, Inc) for immunoprecipitation of GFP-rab5. The [<sup>32</sup>P]GTP was visualized in autoradiography cassettes containing intensifying screens by exposing at –80°C for 18 hours.

### Calculation of diffusion coefficient for GFP-rab5:Q79L

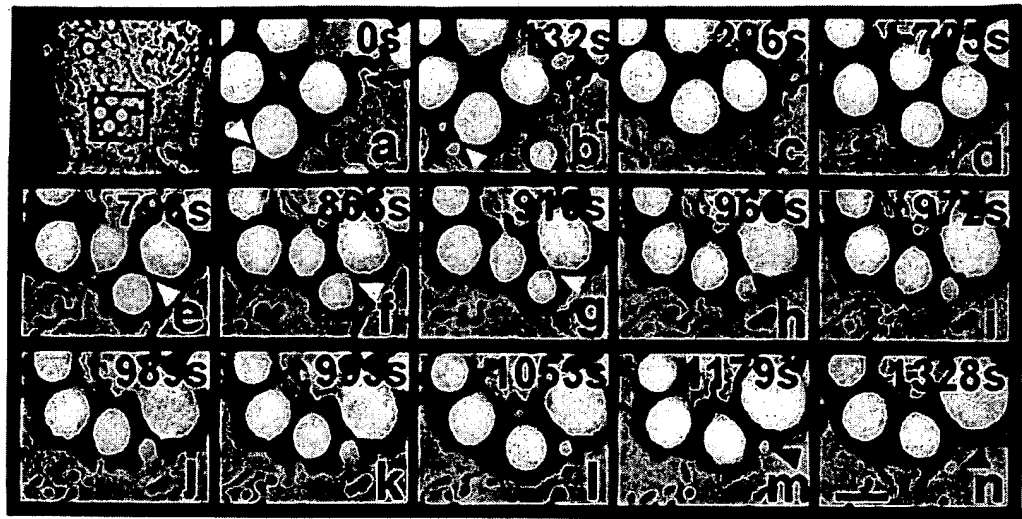
Cells overexpressing GFP-rab5:Q79L were viewed by confocal microscopy at room temperature and inspected for fusion couplets with pairs of docked endosomes 1–3  $\mu$ m in diameter. The fusion couplets were centered and the adjustable laser field was made smaller until only a small part of one endosome of the fusion pair was included in the field. This portion of the endosomal membrane was scanned 2 or 3 times at 100% laser power which resulted in the immediate reduction of fluorescence intensity of the entire photobleached endosome membrane to background levels nearly equivalent to the fluorescence intensity of cytosol. Following photobleaching, the laser field was returned to the normal size and the photobleached fusion couplets were recorded over time. A number of recordings included 'explosive' fusion events between bleached and unbleached endosomes and the diffusion coefficient of GFP-rab5 on endosomes was determined from the average of 4 of these events. See Appendix for a detailed description of the methods used to calculate the GFP-rab5 diffusion coefficient.

## RESULTS

### Giant endosome fusion occurs mostly by a 'bridge' fusion mechanism: time-lapse video microscopy

We have taken advantage of the giant endosomes that develop in cells overexpressing a constitutively active rab5 mutant (rab5:Q79L) (Stenmark et al., 1994) to directly monitor endosome fusion by video microscopy. TRvb1 cells and BHK cells were infected with recombinant Sindbis virus encoding rab5:Q79L, as described previously (Li and Stahl, 1993) and examined by phase contrast microscopy. The Sindbis virus expression system resulted in about a 5-fold overexpression of rab5 protein as judged by western blotting, compared to control cells. At about 3 hours post infection numerous tiny, phase-bright cytoplasmic vesicles became discernible. Over time these vesicles increased in size and by 4–6 hours post-infection

**Fig. 1.** TRvb1 cells overexpressing rab5:Q79L recorded by phase contrast video microscopy. Photomicrographs show a cluster of docked endosomal vesicles that, over time, participate in multiple 'bridge' fusion events. Note that the final 'bridge' fusion event depicted is incomplete and results in one giant vesicle as well as one tiny vesicle (arrowheads in m and n). Relative times in seconds are shown. Bar, 2  $\mu$ m.



many 1-2  $\mu$ m diameter cytoplasmic vesicles were present. These vesicles show strong immunoreactivity for rab5 and are positive for internalized rhodamine-transferrin (data not shown). Comparably enlarged endosomes occur in many cells overexpressing rab5:wt.

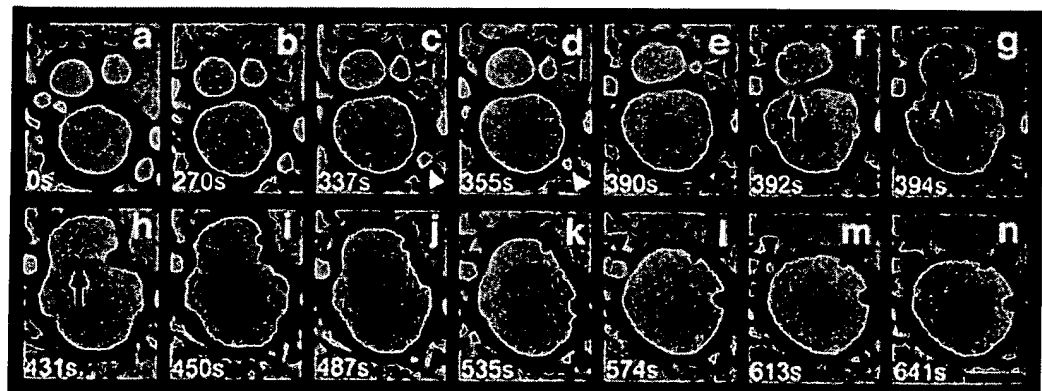
Video microscopy of TRvb1 and BHK cells overexpressing either wild type or rab5:Q79L revealed that endosome fusion occurs by two distinct mechanisms, 'bridge' and 'explosive' fusion. In 'bridge' fusion, one of a pair of 'docked' vesicles gradually decreases in diameter while the companion vesicle gradually increases in diameter, apparently due to the slow transfer of membrane from one to the other (Fig. 1). Invariably in such events, the vesicle that starts off smaller ends up being consumed by the larger, most likely due to differences in surface tension. Distinct from 'bridge' fusion is a type of fusion termed 'explosive' fusion in which the fusion pore that forms between docked endosomal vesicles expands rapidly (Fig. 2). In 'explosive' fusion there is a rapid coalescence of vesicle membrane and an abrupt formation of a single, enlarged luminal compartment. In 'bridge' fusion membrane merger proceeds slowly, often requiring up to 1 to 2 minutes, and the transfer of membrane from the donor to the acceptor endosomal vesicle appears to occur entirely through a very

narrow 'bridge' between fusion couplets. This unusual form of coalescence is the predominant mechanism of vacuole fusion in cells overexpressing both forms of rab5 as it occurred in 81% of the fusion events in cells overexpressing the constitutively active rab5 mutant (rab5:Q79L) and 62% of the fusion events in cells overexpressing wild-type rab5. Rarely (in 5% of 'bridge' fusion events) vacuole coalescence was incomplete, in that fusion was terminated by the disengagement of the endosomes before the donor vesicle had been completely consumed (arrows in Fig. 1m,n).

#### Overexpression of GFP-rab5 fusion proteins results in enlarged fluorescent endosomes

We next utilized GFP fusion proteins, including GFP-rab5:wt and GFP-rab5:Q79L, in order to localize rab5 during the docking and fusion reactions in living cells. The GFP-rab5 proteins both migrated with a molecular mass of approximately 50 kDa following SDS-PAGE (Fig. 3a). The GFP-rab5 fusion proteins were shown to bind [ $^{32}$ P]GTP and this binding was greatly diminished in competition experiments where excess unlabeled GTP was included in the reaction mixture (Fig. 3b). GFP-rab5 proteins were similarly prenylated as compared to native rab5 as judged by the incorporation of tritiated mevalonolactone as

**Fig. 2.** TRvb1 cell overexpressing rab5:Q79L recorded by phase contrast video microscopy. Photomicrographs show a cluster of giant vesicles that over time show multiple fusion events. The sequence begins with two 'bridge' fusion events (black arrowheads, b,c,d; white arrowheads, c,d). Arrowheads point to donor vesicles in fusion couplets that show gradual reduction in diameter with incorporation into larger, acceptor vesicles. An 'explosive' fusion is shown in f through l. In 'explosive' fusion the 'fusion pore' rapidly enlarges (arrows, f,g,h). A third 'bridge' fusion event is also displayed (arrowheads, j,k,l,m). Relative times in seconds are shown. Bar, 2  $\mu$ m.



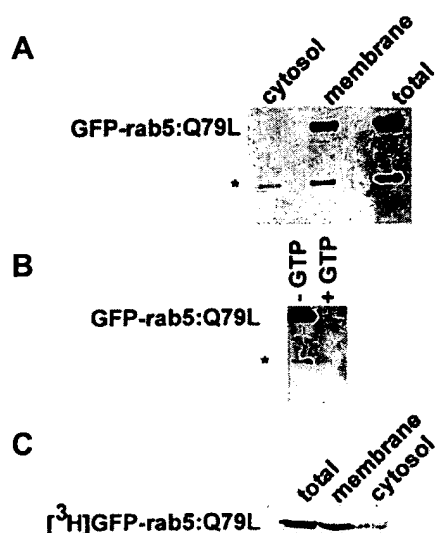


**Fig. 3.** (A) BHK cells overexpressing GFP-rab5:Q79L were fractionated and rab5 immunoreactivity in post-nuclear membrane fractions and cytosol are shown. Here, the endogenous rab5 (\*) migrates with a molecular mass of approximately 24,000 daltons, whereas GFP-rab5:Q79L migrates at approximately 50,000 daltons. (B) Blot showing [ $^{32}$ P]GTP binding. Immunoprecipitates from BHK cells overexpressing GFP-rab5:Q79L were prepared and following SDS-PAGE and were tested for [ $^{32}$ P]GTP binding. In the absence of unlabeled GTP (left lane, [-GTP]), strong [ $^{32}$ P]GTP binding was detected at 50,000 daltons corresponding to overexpressed GFP-rab5:Q79L. A weaker signal was detected at about 24,000 daltons corresponding to [ $^{32}$ P]GTP binding by endogenous rab5 (\*). [ $^{32}$ P]GTP binding was greatly reduced when excess unlabeled GTP was included in the reaction mixture (right lane, [+GTP]). (C) Prenylation of GFP-rab5:Q79L in living BHK cells was detected by incorporation of tritiated mevalonolactone. Radiolabelled BHK cells were fractionated as described above and proteins separated by SDS-PAGE. The major labeled band occurred at about 50000 daltons corresponding to overexpressed GFP-rab5:Q79L.

described by Alvarez-Dominguez et al. (1996) (Fig. 3c). BHK and TRvbl cells overexpressing a GFP-rab5:Q79L fusion protein developed giant cytoplasmic vesicles that show green fluorescence over their entire surface. Nearly all of these were also strongly positive for transferrin receptor, a marker of early endosomes (data not shown). Cells overexpressing GFP-rab5:wt also exhibited fluorescent cytoplasmic vesicles that also colocalize with transferrin receptor, however, in most cells the fluorescent vesicles were smaller than those in cells overexpressing the active rab5 mutant, ranging in size from 0.2–0.5  $\mu$ m in maximal diameter. Occasional cells, however, did contain clusters of giant endosomes. There was no appreciable labeling of the surface membrane in cells overexpressing GFP-rab5:wt or GFP-rab5:Q79L. The Sindbis virus expression system resulted in about a 5-fold overexpression of GFP-rab5 compared to endogenous levels of rab5 protein as judged by western blotting (see Fig. 3a).

#### Endosome docking is accompanied by the recruitment of rab5 into a highly fluorescent spot between fusion couplets

Confocal microscopy demonstrated that docking and fusion of

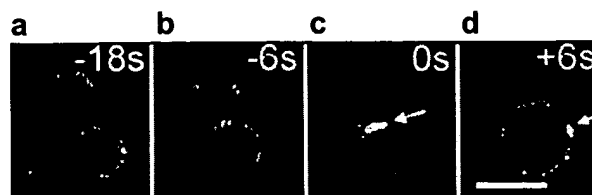


**Fig. 4.** BHK cells overexpressing GFP-rab5:Q79L. Sequence shows an endosome docking reaction and an 'explosive' fusion event. The time interval between frame b and c is six seconds. Note that the vesicles make contact in b without an increase in pixel intensity in the 'bridge' region while in c (six seconds later) there is a nearly 3-fold fluorescence intensity increase in the 'bridge' region compared to the rest of the membrane. Bar, 1.2  $\mu$ m.

giant endosomal vesicles involved recruitment of rab5 into the 'bridge' region between them as cells overexpressing GFP-rab5 fusion proteins (both wild type and Q79L) developed a brightly fluorescent spot at the point where fusing endosomes contact (Figs 4, 5, 6 and 8a). In cells overexpressing GFP-rab5:Q79L the pixel intensity in spots ranged from 2.5–8.0 times the pixel intensity in regions of the endosome membranes away from the 'bridge' region. The mean pixel intensity in GFP-rab5:Q79L spots averaged  $3.4 \pm 0.5$  times the pixel intensity of endosomal membranes away from the 'bridge' region of fusion couplets. In cells overexpressing GFP-rab5:wt the pixel intensity in spots averaged  $2.7 \pm 0.4$  times the pixel intensity of endosomal membranes away from the 'bridge' region of fusion couplets. These spots occurred in 96% of fusion events in cells overexpressing GFP-rab5:Q79L and in 80% of fusion events in cells overexpressing GFP-rab5:wt. In most instances, the spots form 6–30 seconds following the initial contact of fusion pairs and appeared equally bright regardless of whether the docked vesicles progressed to 'bridge' or 'explosive' fusion. We found

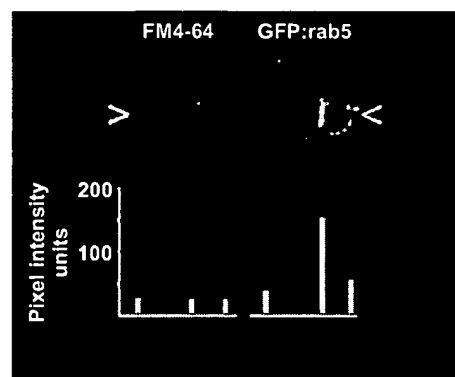


**Fig. 5.** A fusion couplet from a BHK cell overexpressing GFP-rab5:Q79L incubated in FM4-64 (2  $\mu$ g/ml) for 30 minutes. The red and green channel were simultaneously recorded and the pixel intensities from various regions with the fusion couplet were determined. The pixel intensity data represent an average of 6 pixels taken from the regions where the endosomal membranes intersect an imaginary line that passes between the arrowheads. In the case of FM4-64 all values are around 30 pixel intensity units, without any increase in the 'bridge' region. This is in contrast GFP-rab5:Q79L where the pixel intensity in the 'bridge' region is 3–4 times higher (131) than areas away from the 'bridge' region (32 and 40).

that in cells overexpressing GFP-rab5:Q79L, greater than 80% of GFP containing spots, defined as focal regions with pixel intensities greater than 2 times the mean membrane pixel intensity, occurred in the region between fusing endosomes (42 of 50 fluorescent spots). Additionally, the fluorescent spots remained intact over relatively long time intervals in both types of fusion. In 'bridge' fusion, the spot remained intact between fusion partners for the entire duration of the fusion event (up to 2 minutes). Moreover, the fluorescent spots persisted in 'explosive' fusion, moving from the zone of initial contact and fusion to a different position on the membrane of the fusion product where it often remained largely intact for extended periods (occasionally up to 5 minutes following fusion, see below). It is impossible to precisely determine the rate of disassembly of rab5-containing spots as these structures often rapidly drift out of the plane of focus. Although marked enlargement of endosomes is not a consistent feature of GFP-rab5:wt overexpression, we have found enlarged endosomes (0.5–1  $\mu\text{m}$ ) in many cells overexpressing GFP-rab5:wt and in these cells the docking reaction is marked by the formation of fluorescent spots similar to those found in cells overexpressing the GFP-rab5:Q79L.

#### The GFP-rab5 spot does not accumulate other endosome membrane markers

In order to compare the intensity of the GFP-rab5 spots to the intensity of other endosomal membrane markers in the 'bridge' region of fusion couplets, cells on glass coverslips overexpressing GFP-rab5:Q79L were incubated in either FM4-64 (4  $\mu\text{g}$  per ml), rhodamine-WGA (2  $\mu\text{g}$  per ml) or rhodamine-transferrin (20  $\mu\text{g}$  per ml) for 30 minutes at 37°C and washed in media containing 10% fetal calf serum. Confocal microscopy demonstrated GFP-rab5:Q79L spots between fusion couplets as described above, however, other membrane components including FM4-64, WGA binding proteins and transferrin receptors were more diffusely present on the endosomal membrane without appreciable concentration in the 'bridge' region (Fig. 5). In the case of FM4-64, the mean pixel intensity in the 'bridge' region was  $1.2 \pm 0.2$  times the average pixel intensity away from the region between fusion couplets. This is evidence that the spots represent GFP-rab5-containing macromolecular assemblies and do not represent non-specific clustering of membrane proteins or the overlap of the membranes of fusing vesicles. Table 1 shows the fold increase in pixel intensity in the 'bridge' region of fusion couplets compared to the pixel intensity of endosomal membranes away from this area.

Another piece of evidence that the GFP-rab5 spots represent a localized accumulation of rab5 and not overlap of adjacent

**Table 1. Fold increase in pixel intensity of 'hot spot' compared to pixel intensity away from 'hot spot' expressed in AU\***

	'Hot spot'
GFP-rab5:wt	$2.7 \pm 0.4$ ( $n=12$ )
GFP-rab5:Q79L	$3.4 \pm 0.5$ ( $n=24$ )
Rhodamine-transferrin	$1.1 \pm 0.1$ ( $n=8$ )
FM4-64	$1.2 \pm 0.2$ ( $n=12$ )

\*The mean pixel intensity of endosomal membranes away from the 'hot spot' is defined as 1 AU (arbitrary unit).

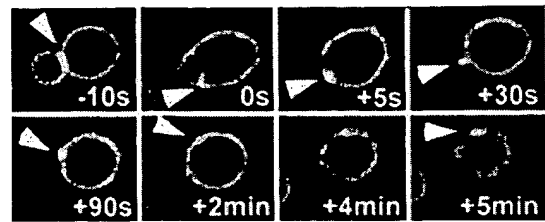


**Fig. 6.** A fusion couplet from a BHK cell overexpressing GFP-rab5:Q79L. There is a 3-fold increase in pixel intensity in 'bridge' region compared to the rest of the membrane. In addition, the spot persists for greater than 5 minutes following the 'explosive' fusion event.

membranes is the persistence of GFP-rab5 spots for up to several minutes following 'explosive' fusion (Fig. 6). Persistence of GFP-rab5:Q79L 'hot spots' occurred in 60% (12 out of 20) explosive fusion events analyzed and occurred in cells expressing GFP-rab5:wt.

#### Rab5 microdomains in endosomal membranes

Finally, we used the confocal laser to photobleach only one of a pair of docked endosomes in a fusion couplet. Photobleaching resulted in a rapid reduction in the fluorescence intensity of the bleached membrane to near background (cytosolic) levels. Furthermore, we found that all of the GFP-rab5:Q79L on the endosomal membrane was rapidly bleached even if only a small portion of the membrane was exposed to the laser. This demonstrates that there is rapid diffusion of GFP-rab5:Q79L throughout the membrane of a single endosome. However, in all of six separate experiments, GFP-rab5:Q79L spots persisted after photobleaching and the mean pixel intensity in the spots remained high; generally greater than 2 times the mean pixel intensity of the non-photobleached membrane (Fig. 7). The persistence of the spots after photobleaching shows that GFP-rab5:Q79L in spots is slow to diffuse into the photobleached membrane and is evidence that the GFP-rab5 spots represents a separate membrane microdomain of docked endosomes.

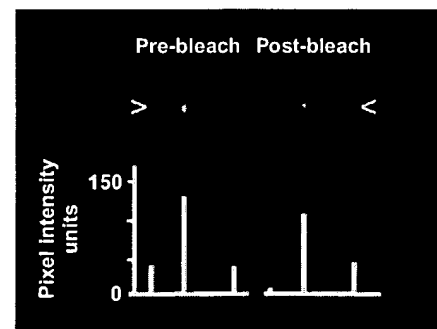


**Fig. 7.** A fusion couplet before (left) and after (right) photobleaching is depicted in a BHK cell overexpressing GFP-rab5:Q79L. The pixel intensity data represent the average of 6–12 pixels taken from the region where the endosomal membranes intersect an imaginary line that passes between the arrowheads. Note that the pixel intensity in the spot remains high (greater than 2-fold over non-'bridge' region) after photobleaching.

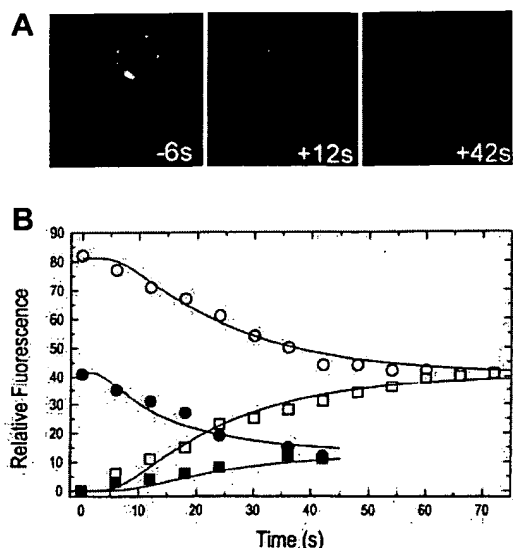


**Fig. 8.** (A) Photobleached fusion couplet in which 'explosive' fusion occurs at  $t=0$  seconds. One portion of the fusion product (top) shows increased fluorescence compared to the bleached portion (bottom). The fluorescence intensities over the entire membrane equalizes over time. (B) Plot shows fluorescence at the poles of a vesicle, formed by the fusion of a bleached and unbleached vesicle, as a function of time. Circles are the fluorescence intensity at the pole of the initially labeled portion and squares are the intensity at the initially unlabeled pole. Filled symbols are data from the fusion event depicted in A, in which the labeled vesicle was the smaller of the two. Open symbols are data when the vesicles were of equal size. A small background fluorescence was subtracted from all the measurements. Solid lines are the best fit of Equation (1) to the data.

Recordings of fusion events between photobleached and unphotobleached endosomes show rapid diffusion of GFP-rab5:Q79L on the endosomal membrane demonstrated by the rapid mixing of photobleached and unphotobleached GFP-rab5:Q79L (Fig. 8a). One to two minutes after these fusion events, the endosomal membrane exhibited a fluorescence intensity that was about midway between the intensity of the unphotobleached and photobleached membranes prior to fusion, given that the fusion partners were of a similar size. We

calculated the diffusion coefficient of GFP-rab5:Q79L to be around  $1.0 (\pm 0.3) \times 10^{-9} \text{ cm}^2/\text{second}$  at room temperature by the method described by Huang (1973; see Figs 8 and 9) using plots that show changes in pixel intensity at the poles of the vesicle over time following fusion. These data were obtained from 4 photobleach experiments that show mixing of photobleached and non-photobleached GFP-rab5:Q79L after 'explosive' fusion events (Fig. 8b). The calculated diffusion constant is in the high range of values for membrane proteins and is similar in magnitude to many GPI-linked membrane proteins (Zhang et al., 1993). GFP-rab5:wt was also found to rapidly diffuse on endosomal membranes (data not shown). Filled symbols in Fig. 8b are data from the fusion event depicted in Fig. 8a in which the fusing vesicles were of different sizes, while open symbols are data where the fusing vesicles were of equal size. These experiments show that most GFP-rab5:Q79L diffuses quite rapidly compared to GFP-rab5:Q79L localized to spots between fusion couplets, which is diffusion resistant.

## DISCUSSION

The presence of giant endosomes in cells overexpressing wild-type rab5 or the GTPase defective mutant of rab5 has provided a unique opportunity to observe and record the behavior of endosomes in living cells. This has led to the observation that endosomes fuse by two apparently different mechanisms that we term 'bridge' fusion and 'explosive' fusion. It appears based on the morphology of GFP-rab5 'hot spots' that the two fusion mechanisms proceed similarly with respect to GFP-rab5, however, the fusion pore dynamics are different. It is possible that the molecular composition of 'hot spots' in the two types of fusion are different. The majority of the fusion events we observed were of the 'bridge' type. The reasons for this are unclear as the initial steps in both types of giant vesicle fusion, including vesicle docking and formation of the GFP-rab5 spot at the docking site, appeared to be the same in both types of fusion. It is possible that disassembly of a rab5 containing docking/fusion complex, present between fusion couplets, is delayed thereby increasing the frequency of 'bridge' fusion events observed in these studies. However, 'bridge' fusion identified in these experiments does not appear to be a consequence of either rab5 overexpression or the Sindbis virus expression system utilized as both types of endosome fusion have been identified in virus-free cells in which endosome enlargement has been induced by exposure to drugs including PMA and chloroquine or hypotonic shock (data not shown). It also appears that contractile vacuole exocytosis in *Dictyostelium* can occur by a mechanism similar to 'bridge' fusion (Heuser et al., 1993) and similar 'bridging' structures have been reported in nuclear membrane fusion in yeast (Kurihara et al., 1994). It is apparent that the 'bridge' mechanism of vesicle fusion described here also shares features with macropinosome-lysosome fusion where fusion events occur gradually, over minutes (Willingham and Yamada, 1978; Racoosin and Sanson, 1995). In both examples the fusion pore between fusion partners remains in a stable, open conformation over time. Also, a number of recent reports have described transient fusion events between different endocytic compartments that result in the retrograde movement of solute from lysosomes to earlier endosomal elements (Berthiaume et

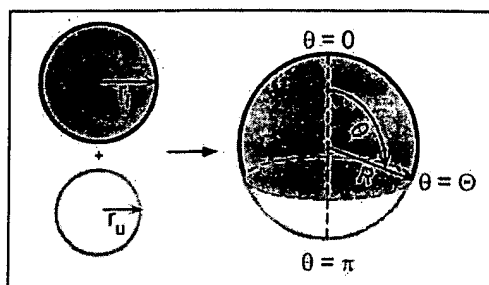


**Fig. 9.** Schematic representation of 'explosive' fusion in which a labeled vesicle (shaded gray) of radius  $r_l$  fuses with a bleached vesicle of radius  $r_u$ . The upper portion of the resulting vesicle (radius  $R$ ) is initially labeled and the lower portion is initially unlabeled. Measurements of fluorescence intensity were made at the poles,  $\theta=0$  and  $\theta=\pi$ .

al., 1995; Wang and Goren, 1987). The finding that fusion events can allow solute mixing to occur, while not resulting in the complete merger of membranes of the different vesicular elements, is further evidence of transient vesicle fusion in which stable open fusion pores must operate.

Most of our understanding of fusion pores is based on electrophysiological studies in model systems of exocytosis (reviewed by Fernandez, 1997 and Monck et al., 1995). These studies have shown that the early fusion pore has conductance properties that correspond to dimensions similar to an ion channel (Spruce et al., 1990); however, the conductance through early fusion pores can vary significantly, presumably due to rapid variations in the diameter of the aqueous channel ('flickering'). Several recent reports have shown that during exocytosis fusion pores routinely exhibit semi-stable, open conformations which are often later followed by abrupt pore closure (Curran et al., 1993; Alvarez de Toledo et al., 1993; Rosenboom and Lindau, 1994; Thomas et al., 1994). In addition, during these incomplete fusion events a significant release of secretory granule contents can occur (Alvarez de Toledo et al., 1993; Lollike et al., 1995). The molecular interactions that delay and/or completely prevent the irreversible expansion of the fusion pore have not been resolved. Also, a recent report characterizing a Baculovirus model system of membrane fusion (Plonsky and Zimmerberg, 1996) has shown stable initial pore conductances consistent with early fusion pores much larger than those previously described in model systems of exocytosis. These features are similar to the 'bridge' fusion pores that also exhibit stable, open conformations for periods of time of up to 2 minutes.

It has been hypothesized that the fusion pore is regulated and defined by a protein scaffold (Monck et al., 1995). This idea originated with electron micrographs of secretory cells that seemed to show cytoplasmic filaments extending between closely opposed plasma membrane and secretory granule membranes (Ornberg and Reese, 1981; Chandler and Heuser, 1980). Subsequently, it was suggested that these filaments might function to deform the membrane into a highly curved cusp or 'dimple' that could increase membrane tension locally and thereby promote fusion (Monck et al., 1995). In artificial membrane systems, increasing membrane tension by increasing lateral tension or membrane curvature increases spontaneous fusion (Helm et al., 1989). Presumably, persistence of such a scaffold could also be important in maintaining such semi-stable fusion pores in their open states. Indeed, the 'bridge' fusion observed here could represent a consequence of the persistence of such a scaffold.

The molecular components of the structures that span the region between vesicles engaged in 'bridge' fusion have not yet been determined although we presume that the 'bridge' complex identified here bears some relation to the macromolecular scaffold identified in electron micrographs of the exocytic fusion pore (Ornberg and Reese, 1981; Chandler and Heuser, 1980) and/or to the SNARE complex of proteins described in biochemical experiments (Söllner et al., 1993). In this study we show that high levels of rab5 are located in the 'bridge' region between fusing endosomes which suggests the participation of a rab5 containing docking/fusion complex in endosome fusion. Rab proteins have not been yet identified in SNARE complexes by biochemical techniques, however, several recent reports suggest that in living cells the

formation of SNARE complexes requires rab protein activity (Sögaard et al., 1994; Johannes et al., 1996).

Five different lines of evidence all support the idea that rab5-containing spots represent specific accumulation of rab5 and not do not represent overlap of adjacent membranes. First, the fluorescence intensity (pixel brightness) in the spots was  $3.4 \pm 0.5$  times the fluorescence intensity of endosomal membranes away from the 'bridge' zone of fusing endosomes. If the fluorescent spots represented membrane overlap then the fluorescence intensity in the spots would be twice the fluorescence intensity away from the spots. The fluorescence intensity of the spots shown in Figs 4, 5, 6, 7 and 8a are all nearly 3- to 4-fold higher than the pixel intensity of endosomal membrane away from the spots. Second, rab5 accumulates in spots while other endosome membrane markers like FM4-64 (Fig. 5) and transferrin (data not shown) do not. If the fluorescent spots were a consequence of membrane overlap, then the intensity of all endosome membrane markers would be 'doubled'. Third, GFP-rab5 containing spots often persist for extended time intervals following fusion (Fig. 6). These spots would disappear immediately following fusion if they represented overlap of adjacent membranes. Fourth, the fluorescent spots persist following photobleaching (Fig. 7). If the GFP-rab5 containing spots corresponded to overlap of two closely associated endosomal membranes, then the spots would be expected to disappear following photobleaching one of the endosomal membranes to background levels because the 'doubling' effect would then be eliminated. In fact, the fluorescence intensity in spots was largely unaffected by the photobleaching. Fifth, as described in the text, GFP-rab5 containing spots are not detected at all sites of contact between adjacent endosomes, but instead are almost always found between endosome fusion couplets.

Some properties of the GFP-rab5 spot have been further explored using the confocal microscope as an instrument to photobleach specific regions of endosomes. We have utilized photobleaching experiments to demonstrate that GFP-rab5 rapidly diffuses on endosomal membranes but that the diffusion of GFP-rab5 located in spots between fusing endosomes is highly restricted and slow. We have shown that that entire endosomes can be uniformly photobleached even when only small portions of the endosomal membranes are exposed to the confocal laser. This result shows that photobleached and non-photobleached GFP-rab5:Q79L rapidly diffuse and mix following exposure to the laser. In addition, recordings of explosive fusion events between photobleached and unphotobleached endosomes show the rapid diffusion and mixing of bleached and unbleached GFP-rab5:Q79L following fusion. Using plots of pixel intensity and the changes in intensity over time following fusion, we have calculated that GFP-rab5:Q79L diffuses at a rate of  $1.0 (\pm 0.3) \times 10^{-9}$  cm<sup>2</sup>/second, a rate similar to that of many GPI-linked proteins (Zhang et al., 1993).

In summary, we have shown that fusion of giant endosomal vesicles in cells overexpressing active rab5 constructs occurs by a mechanism in which the fusion pore between fusion partners remains open for extended periods of time. In addition, in cells expressing GFP-rab5 constructs the vesicle docking reaction is associated with the formation of a rab5-containing spot between fusion partners which persists for extended time intervals following fusion.



## APPENDIX

## Calculation of diffusion coefficient of GFP-rab5:Q79L on endosomal membranes

To calculate the diffusion constant of GFP-rab5:Q79L, we assume that immediately following fusion ( $t=0$ ), two docked vesicles form a single spherical vesicle in which part of the surface is labeled uniformly with GFP-rab5:Q79L while the photobleached membrane is essentially unlabeled and exhibits a fluorescence intensity similar to that found in the cytosol. Following fusion the unbleached GFP-rab5:Q79L diffuses onto the photobleached part of the surface while photobleached GFP-rab5:Q79L diffuses onto the non-photobleached portion. Over time (up to 2 minutes), the fluorescence intensities equalize over the entire surface. For the calculation of the diffusion coefficient we assume a vesicle of radius  $r_l$  labeled with GFP-rab5 fuses with an unlabeled (photobleached) vesicle of radius  $r_u$  forming a vesicle of radius  $R=\sqrt{r_l^2+r_u^2}$  (Fig. 9). We assume that initially ( $t=0$ ) a single spherical vesicle is formed with part of its surface labeled uniformly with GFP-rab5:Q79L and the rest unlabeled. The labeled surface is specified by polar angle  $0\leq\theta\leq\Theta$  and the unlabeled surface by  $\Theta<\theta<\pi$ , where

$$\Theta = \cos^{-1}\left(1 - 2 \frac{r_l^2}{R^2}\right)$$

(Fig. 9). After fusion the protein diffuses onto the unlabeled portion of the sphere.

The concentration of the labeled protein as a function of position and time is given by the general solution of the diffusion equation for a spherical surface (e.g. Huang, 1973):

$$c(x,t) = \sum_{l=0}^{\infty} A_l P_l(x) \exp\left[-\frac{D}{R^2} l(l+1)t\right], \quad (1)$$

where  $c(x,t)$  is the concentration of the diffusing species at time  $t$  and position  $x$ ,  $x=\cos\theta$  ( $-1\leq x\leq 1$ ),  $P_l(x)$  are Legendre polynomials,  $D$  is the diffusion coefficient,  $R$  is the radius of the sphere, and  $A_l$  are arbitrary constants determined by the initial conditions. At  $t=0$ , Equation (1) reduces to

$$c(x,0) = \sum_{l=0}^{\infty} A_l P_l(x). \quad (2)$$

For  $x\leq\cos\Theta$ ,

$$c(x,0) = c_e \frac{r_l^2 + r_u^2}{r_l^2},$$

and for  $x\geq\cos\Theta$ ,  $c(x,0)=0$ , where  $c_e$  is the final, equilibrium concentration. The sum in (2) is a Fourier series in which the  $P_l(x)$  make up an orthonormal set of functions over the interval  $(-1,1)$  with respect to the weight function

$$r(x) = \frac{2l+1}{2},$$

i.e.

$$\int_{-1}^1 P_m(x) P_n(x) r(x) dx = \begin{cases} 0 & \text{for } m \neq n \\ 1 & \text{for } m = n \end{cases} \quad (3)$$

The  $A_l$  are then calculated by multiplying (2) by  $P_l$ , integrating from  $-1$  to  $1$ , and applying the properties of (3). This procedure yields

$$A_l = c_e \frac{2l+1}{2} \frac{r_l^2 + r_u^2}{r_u^2} \int_{\cos\Theta}^1 P_l(x) dx, \quad (4)$$

where  $Z \equiv \cos\Theta$ .

A Mathcad (MathSoft, Inc.) program was written to calculate the Legendre polynomials, the coefficients  $A_l$ , and find the best fit (by a least-squares criterion) of Equation (1) to the experimental variation in concentration at the poles by varying the values of the diffusion coefficient,  $D$ , and the equilibrium concentration,  $c_e$ .

We thank Rita Boshans for her assistance in generating the GFP constructs and Cheryl Adles for assistance with tissue culture. We thank Elliot Elson for his oversight in the calculation of the diffusion coefficient of GFP-rab5:Q79L and John Heuser, Marisa Colombo, Elliot Elson, and Paul Schlesinger for critically reading the manuscript.

## REFERENCES

- Alvarez de Toledo, G., Fernandez-Chacon, R. and Fernandez, J. M. (1993). Release of secretory products during transient vesicle fusion. *Nature* **363**, 554-558.
- Alvarez-Dominguez, C., Barbieri, A. M., Beron, W., Wandinger-Ness, A. and Stahl, P. D. (1996). Phagocytosed live *Listeria monocytogenes* influences Rab5-regulated in vitro phagosome-endosome fusion. *J. Biol. Chem.* **271**, 13834-13843.
- Barbieri, M. A., Li, G., Mayorga, L. S. and Stahl, P. D. (1996). Characterization of Rab5:Q79L-stimulated endosome fusion. *Arch. Biochem. Biophys.* **326**, 64-72.
- Berthiaume, E. P., Medina, C. and Swanson, J. A. (1995). Molecular size fractionation during endocytosis in macrophages. *J. Cell Biol.* **129**, 989-998.
- Broadie, K., Prokop, A., Bellen, H., O'Kand, C. J., Schulze, K. L. and Sweeney, T. S. (1995). Syntaxin and synaptobrevin function downstream of vesicle docking in *Drosophila*. *Neuron* **15**, 663-673.
- Chandler, D. E. and Heuser, J. E. (1980). Arrest of membrane fusion events in mast cells by quick freezing. *J. Cell Biol.* **86**, 666-674.
- Cole, N. B., Smith, C. L., Seiky, N., Terasaki, M., Edidin, M. and Lippincott-Schwartz, J. (1996). Diffusional mobility of Golgi proteins in membranes of living cells. *Science* **273**, 797-801.
- Curran, M. J., Cohen, F. S., Chandler, D. E. and Zimmerberg, J. (1993). Exocytotic fusion pores exhibit semi-stable states. *J. Membr. Biol.* **133**, 61-75.
- Diaz, R., Mayorga, L. and Stahl, P. (1988). In vitro fusion of endosomes following receptor-mediated endocytosis. *J. Biol. Chem.* **263**, 6093-6100.
- Fernandez, J. M. (1997). Cellular and molecular mechanics by atomic force microscopy: Capturing the exocytotic fusion pore in vivo? *Proc. Nat. Acad. Sci. USA* **94**, 9-10.
- Gruenberg, J. and Maxfield, F. R. (1995). Membrane transport in the endocytic pathway. *Curr. Biol.* **7**, 552-563.
- Hay, J. C. and Scheller, R. H. (1997). Snares and NSF in targeted membrane fusion. *Curr. Opin. Cell Biol.* **9**, 505-512.
- Heim, R., Prasher, D. C. and Tsien, R. Y. (1994). Wavelength mutations and posttranslational autooxidation of green fluorescent protein. *Proc. Nat. Acad. Sci. USA* **91**, 12501-12504.
- Helm, C. A., Israilachvili, J. N. and McGuiggan, P. M. (1989). Molecular mechanisms and forces involved in the adhesion and fusion of amphiphilic bilayers. *Science* **245**, 919-922.
- Heuser, J., Zhu, Q. and Clarke, M. (1993). Proton pumps populate the contractile vacuoles of *Dictyostelium amoebae*. *J. Cell Biol.* **121**, 1311-1327.
- Huang, W. W. (1973). Mobility and diffusion in the plane of the membrane. *J. Theor. Biol.* **40**, 11-17.
- Hunt, J. M., Bommert, K., Charlton, M. P., Kistner, A., Habermann, E., Augustine, G. J. and Betz, H. (1994). A post-docking role for synaptobrevin in synaptic vesicle fusion. *Neuron* **12**, 1269-1279.
- Johannes, L., Doussau, A., Clabecq, A., Henry, J.-P., Darchen, F. and



- Poulain, B. (1996). Evidence for a functional link between Rab3 and the SNARE complex. *J. Cell Sci.* **109**, 2875-2884.
- Kurihara, L. J., Beh, C. T., Latterich, M., Schekman, R. and Rose, M. D. (1994). Nuclear congression and membrane fusion: two distinct events in the yeast karyogamy pathway. *J. Cell Biol.* **126**, 911-923.
- Lewis, W. H. (1931). Pinocytosis. *Bull. Johns Hopkins Hosp.* **49**, 17-36.
- Li, G. and Stahl, P. D. (1993). Structure-function relationship of the small GTPase Rab5. *J. Biol. Chem.* **268**, 24475-24480.
- Lollike, K., Borregaard, N. and Lindau, M. (1995). The exocytotic fusion pore of small granules has a conductance similar to an ion channel. *J. Cell Biol.* **129**, 99-104.
- Monck, J. R., Oberhauser, A. F. and Fernandez, J. M. (1995). The exocytotic fusion pore interface: a model of the site of neurotransmitter release. *Mol. Membr. Biol.* **12**, 151-156.
- Novick, P. and Zerial, M. (1997). The diversity of rab protein in vesicle transport. *Curr. Opin. Cell Biol.* **9**, 496-504.
- Ornberg, R. L. and Reese, T. S. (1981). Beginning of exocytosis captured by rapid-freezing of limulus amebocytes. *J. Cell Biol.* **90**, 40-54.
- Plonsky, I. and Zimmerberg, J. (1996). The initial fusion pore induced by baculovirus GP64 is large and forms quickly. *J. Cell Biol.* **135**, 1831-1840.
- Racoosin, E. L. and Sanson, J. A. (1993). Macropinosome maturation and fusion with tubular lysosomes in macrophages. *J. Cell Biol.* **121**, 1011-1020.
- Rosenboom, J. and Lindau, M. (1994). Exo-endocytosis and closing of the fission pore during endocytosis in single pituitary nerve terminals internally perfused with high calcium concentration. *Proc. Nat. Acad. Sci. USA* **91**, 5267-5271.
- Rothman, J. E. and Warren, G. (1994). Implications of the SNARE hypothesis for intracellular membrane topology and dynamics. *Curr. Biol.* **4**, 220-233.
- Simons, K. and Zerial, M. (1993). Rab proteins and the road maps for intracellular transport. *Neuron* **11**, 789-799.
- Sögaard, M., Tani, K., Ye, R. R., Geromanos, S., Tempst, P., Kirchhausen, T., Rothman, J. E. and Söller, T. (1994). A Rab protein is required for the assembly of SNARE complexes in the docking of transport vesicles. *Cell* **78**, 937-948.
- Söller, T., Whiteheart, S. W., Brunner, M., Erdjument-Bromage, H., Geromanos, S., Tempst, P. and Rothman, J. E. (1993). SNAP receptors implicated in vesicle targeting and fusion. *Nature* **362**, 318-324.
- Spruce, A. E., Breckenridge, L. J., Lee, A. K. and Almers, W. (1990). Properties of the fusion pore that forms during exocytosis of a mast cell secretory vesicle. *Neuron* **4**, 643-654.
- Stenmark, H., Parton, P. G., Steele-Mortimer, O., Lutcke, A., Gruenberg, J. and Zerial, M. (1994). Inhibition of Rab5 GTPase activity stimulates membrane fusion in endocytosis. *EMBO J.* **13**, 1287-1296.
- Thomas, P., Lee, A. K., Wong, J. G. and Almers, W. (1994). A triggered mechanism retrieves membrane in seconds after  $\text{Ca}^{++}$ -stimulated exocytosis in single pituitary cells. *J. Cell Biol.* **124**, 667-675.
- Wang, W.-L. and Goren, M. B. (1987). Differential and sequential delivery of fluorescent lysosomal probes into phagosomes in mouse peritoneal macrophages. *J. Cell Biol.* **104**, 1749-1754.
- Weber, T., Zemelman, B. V., McNew, J. A., Westermann, B., Gmachl, M., Parlati, F., Söller, T. H. and Rothman, J. E. (1998). SNAREpins: minimal machinery for membrane fusion. *Cell* **92**, 759-772.
- Willingham, M. C. and Yamada, S. S. (1978). A mechanism for the destruction of pinosomes in cultured fibroblasts: piranha lysis. *J. Cell Biol.* **78**, 480-487.
- Zhang, F., Lee, G. M. and Jacobson, K. (1993). Protein lateral mobility as a reflection of membrane microstructure. *BioEssays* **15**, 579-588.